Academic Sciences International Journal of Pharmacy and Pharmaceutical Sciences

ISSN- 0975-1491 Vol 6 Issue 2, 2014

Research Article

# STABLE COLLOIDAL CHITOSAN/ALGINATE NANOCOMPLEXES: FABRICATION, FORMULATION OPTIMIZATION AND REPAGLINIDE LOADING

**ENAS ELMOWAFY, RIHAB OSMAN*, ABD EL-HAMEED A. EL-SHAMY, GEHANNE AS AWAD**

**Department of Pharmaceutics and Industrial Pharmacy, Faculty of Pharmacy, Ain Shams University, African organization unity street, Cairo, Egypt. Email: rihabosman@pharma.asu.edu.eg**

*Received: 03 Feb 2014, Revised and Accepted: 13 Mar 2014*

**ABSTRACT**

Objective: The objective of the present work was to optimize the formulation of chitosan/alginate nanocomplexes (CS/ALG NCs) and to evaluate the effect of the amphoteric drug, repaglinide (REP), loading on NCs properties.

Methods: CS/ALG NCs were prepared by ionic gelation of chitosan (CS) using sodium alginate (ALG). The effects of CS volume, and pH as well as ALG to CS mass ratio on the particle size and zeta potential of plain NCs were examined. Loading of NCs was achieved using the amphoteric drug, REP. The plain and loaded NCs were characterized using FT-IR, dynamic light scattering and transmission electron microscopy. REP dispersion and crystallographic properties in the cores of NCs were also elucidated using differential scanning calorimetry and X-ray diffraction.

Results: The particle size of CS/ALG NCs and REP-loaded CS/ALG NCs was less than 400 nm with positive surface charge and spherical shape. REP loading and concentration influenced particle size (PS) as well as REP association within NCs matrices. By increasing the mass ratio of ALG to CS to 1:2.5 and fixing REP content at its low level, stable NCs with an appropriate PS of 299 nm and maximum EE% (85%) could be reached. REP was encapsulated as a molecular dispersion in CS/ALG NCs.

Conclusion: The developed CS/ALG NCs may offer a good platform for the mucosal delivery of the insulinotropic drug, REP, overcoming the major drawbacks of its oral delivery.

**Keywords:** Chitosan, Nanocomplexes, Repaglinide, Ionic gelation, Alginate.

## INTRODUCTION

Among the various mucoadhesive polymers, chitosan (CS) and alginate (ALG) are extensively used in biomedical and pharmaceutical applications due to their biocompatibility, low toxicity, biodegradability added to their mucoadhesive power [1]. CS is a polycationic polymer consisting of ß-(1-4)-2-acetamido-2-deoxy-ß-D-glucopyranose and 2-amino-2-deoxy-b-D-glucopyranose, with a pKa value of 6.3–6.5 [2]. Its mucoadhesive properties have been attributed mainly to an interaction between its positively charged amino groups with negatively charged sialic acid groups on the mucus membrane [3]. Its reported capacity to transiently open the tight junctions has been associated with an interaction of chitosan with the Protein Kinase C pathway [4]. In spite of the wide variations of available molecular weights, the low molecular weight CS has shown evidence of better solubility, biocompatibility, biodegradability and lower toxicity compared to the high molecular weight [5]. ALG is a polyanionic linear block copolymer of (1-4)-linked *β*-D-mannuronic acid (M residues) and its C5 epimer, α-L-guluronic acid (G residues), and is usually presented as the sodium salt [1].

The interactions between ALG and CS via their ionizable groups result in the spontaneous production of homogenous, non-toxic and organic-solvent free nanocomplexes (NCs) with controllable size and satisfactory incorporation capacity for various therapeutic agents [6]. The size, drug entrapment and controlled release depend on a number of factors, which include, but are not limited to, polyelectrolytes concentrations, mixing ratio, ionic strength of the solution, mixing order, and pH [7]. The properties of the incorporated drug and especially its pka can also have pronounced effect on the NCs attributes [6].

Mucoadhesive nanoparticles (NPs), receive much attention nowadays due to their ability to deliver various drugs and macromolecules via the nasal route. These NPs strongly attach to the mucosa, decreasing the nasal mucociliary clearance rate and increasing the residence time of the formulation in the nasal cavity, surmounting thus the main challenges to nasal delivery [8]. Moreover, they have the ability to cross the mucosal epithelium not only through the microfold (M) cells overlaying the mucosal associated lymphoid tissue (MALT) but also through the epithelial cells [9]. Literature survey revealed that reduction of NPs size to typically between 50-400 nm could enhance their potential mucosal transcellular uptake, although 100 to 300 nm have been found more suited to the purpose [10]. In addition, demanded cytological response of NPs in terms of cellular uptake rate and amount and intracellular trafficking is highly correlated with their surface charge. Positively charges NPs exhibited better cellular uptake as compared to the negatively and neutrally charged ones [11].

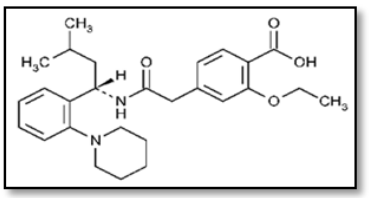


**Fig. 1: Chemical Structure of REP**

Repaglinide (REP), a carbamoyl methyl benzoic acid derivative (Fig. 1), with two pka values of 4.19 and 5.78 [12], was selected for this work. This drug mimics physiological glucose-stimulated insulin release, acting as efficient insulin secretagogue. The drug is capable of controlling both postprandial blood glucose level (PBG) and fasting blood glucose level (FBG) [13], thereby minimizing the risk of diabetes associated complications like macro and microvascular disease through the reduction of oxidative stress, a potent contributor of vascular dysfunction [14]. It is currently delivered only as oral tablets in spite of its short plasma half-life (<1 h) and low bioavailability of about 50% resulting from extensive first pass metabolism [15]. The nasal route, with its large surface area, extensive vascularization, avoidance of first pass effect, ease of administration and applicability for long-term treatment, may give a chance for improving drug bioavailability.

Thus, the ultimate goal of this work was to optimize the formation of CS/ALG- NCs which were further loaded with REP. The formulation variables were changed to manipulate the preparation in order to gain control over the particle size to be suitable for mucosal uptake.

The NCs formation was elucidated via various physico-chemical and morphological characterization tools.

## MATERIALS AND METHOD

### Materials

Chitosan (CS) low molecular weight, (viscosity 9 cP) kindly supplied by Primex Co. (Iceland). Sodium alginate (ALG) was gifted by Memphis, Cairo, Egypt. Repaglinide (REP), kindly provided by EIPICO, Cairo, Egypt. Ultrapure water (MilliQ Plus, Millipore Iberica, Spain) was used throughout. All other materials and reagents used in this study were of analytical grade.

### Methods

#### Preliminary screening study and preparation of plain and REP-loaded CS/ALG NCs

The particles were prepared based on the ionic gelation of CS with ALG. In this method, various amounts of CS and ALG were dissolved in 0.25% acetic acid solution and deionized water respectively and filtered using 0.45 µm syringe filters (Millipore, USA). Slow dripping of ALG solution into the corresponding CS solution was done while stirring, at room temperature.

The suspension, obtained after 15 min stirring, was centrifuged on a 10 µl glycerol layer (15,000xg, 30 min, 25°c) (Hermle Labortechnik GmBH, model Z216MK, Germany). The obtained sediment was resuspended in 100 µl of water, freeze dried and used for subsequent DSC and FTIR studies. Different solution pHs were obtained by mixing CS solutions with various amounts of sodium hydroxide (1N). REP-loaded NCs were prepared by dissolving the drug in the least possible volume of 0.1N NaOH, prior to mixing with anionic ALG solution where the pH was kept at 6.5 (0.025 or 0.05 mg/mLmL REP of final dispersion ) then ALG-drug solution was dripped into CS solution at pH 5 and the NCs were prepared as previously explained.

#### NCs characterization

#### Particle size (PS) determination

The dynamic light scattering technique was used to determine the average hydrodynamic diameter and polydispersity index (PI) of the particles in the freshly prepared dispersions using a Zetasizer® Nano-ZS (Malvern instruments, Malvern, UK). The analysis was performed at 25°C using a scattering angle of 173°.

#### Zetapotential (ζ) determination

Determination of **ζ** potential of each NCs dispersion was performed in a capillary cell using the Malvern Zetasizer equipped with a 4 mW He-Ne laser at a wavelength of 633 nm at 25ºC.

#### Entrapment efficiency percent (EE %)

The supernatant was analyzed using a UV spectrophotometer (UV-1601 PC, Shimadzu, Kyoto, Japan) at λ243nm and the drug EE% was calculated as follows:

$$EE\% = \left[ (total\ REP - free\ REP) \Big/ total\ REP \right] \times 100$$

#### Morphological examination of CS/ALG NCs

The morphological characteristics of NCs were examined using high resolution transmission electron microscopy (HR-TEM). For HR-TEM, a drop of each NCs dispersion was placed on a carbon-film covered copper grid (200 mesh). The sample was then air-dried before observation by high resolution TEM (Jeol, Japan) operating at 200 kV.

#### Thermal analysis by differential scanning calorimetry (DSC)

The thermal properties of REP, CS, ALG, their physical mixture, selected NCs were investigated using DSC (DC-60, Shimadzu, and Kyoto, Japan). An accurately measured amount of each sample (3-5mg) was sealed in an aluminium pan with a lid and was heated at a rate of 10ºC/min to a temperature of 300ºC, using dry nitrogen as carrier gas at a flow rate of 30 mL/min.

#### Crystallographic study by X-ray powder diffraction (XRPD)

XRPD was used to determine the presence of crystalline and amorphous content in selected NCs. A Philips PW 3710 XRPD was used to analyze the formulations, running at 45 kV, 30 mA, and scanning from angles of 5–45°. XRPD patterns of REP, CS, ALG and REP- loaded NCs were obtained.

#### Fourier transform infrared (FT-IR) spectroscopy

FT-IR spectra of REP, CS, ALG, their physical mixture, plain and REP-loaded NCs were recorded with an FT-IR spectrometer (Nicolet 6700 FT-IR; Thermal Scientific; Class 1 laser product; USA) using KBr disc method. All spectra were recorded from 4000 to 400 $cm^{-1}$ at a resolution of 4 $cm^{-1}$ and 16 times scanning for each measurement to obtain an adequate signal to-noise ratio.

#### Colloidal stability

The stability of the selected freshly prepared colloidal CS/ALG NCs dispersions was evaluated by determination of PS and PI after storage at 4 ◦C for one week.

#### Statistical analysis:

Three batches of NCs were prepared for each formulation. The results are expressed as mean ± S.D. The statistical significance of differences was assessed using Student's *t-test* and ANOVA and was termed significant when (P) ≤ 0.05.

## RESULTS AND DISCUSSION

#### Optimization of plain NCs formulations

Aiming at achieving optimized colloidally stable NCs, in terms of PS, PI and **ζ** prior to drug loading, formulae P1 to P8 were prepared. Firstly the optimum volume ratio between the two polymer solutions was determined by studying formulae P1, P2 and P3. Secondly, the optimum pH was chosen by preparing formulae P2, P4 and P5. Finally more optimization was done by studying formulae P6 to P8 in order to determine the optimum mass ratio of both polyelectrolytes. Table 1 shows the composition and characterization of the prepared formulae.

#### CS solution volume effect

In order to determine the NCs formation zone, a fixed volume (1mL) of 0.6 mg ALG was dripped in different volumes containing 0.5 mg/mL of CS at pH 5. At 1:2 volume ratio ALG to CS, no visible opalescence occurred indicating inadequacy of CS amounts for producing a cross-linked structure. At 1:3 volume ratio, a colloidal dispersion was obtained, denoting cross linking. Further increase in CS volume resulted in aggregate formation. The high CS charge density led to large aggregates having a low stability with a high precipitation tendency [16]. Hence, a volume ratio of 1:3 (ALG to CS) was found optimum and was used throughout the study.

#### Cs solution pH effect

ALG, prepared at pH 6.5, was dripped into CS solutions with three pH values: 5, 5.5 and 6 using a volume ratio of 1:3 ALG to CS. The PS was found to increase by raising CS solution pH as seen in table 1. This can be attributed to the variation in degree of CS protonation [16]. A pH closer to the pKa of CS (6.5) causes less protonation for its amino group thus, decreasing the potential of its cross-linking with ALG resulting in larger less dense NCs. Previous investigators reported also higher yields of CS/ ALG matrices at pH 5. They owed this observation to the high availability of ionized carboxylic acid groups on the alginate surface in addition to the increase of CS protonation [17].

#### ALG to CS mass ratio effect

After localizing the NCs formation zone, it deemed necessary to study the effect of varying the polyelectrolytes mass ratio on NCs properties. As seen in table 1, increasing CS content (mass ratio from 1:0.6 to 1:2.5), caused PS dramatic decrease from 359.5 to 259.8 nm which remained almost constant in case of mass ratio 1:5. However, further increase in CS content (P8) led to larger particles again. This means that higher PS values were noticed

with the extremes of mass ratio of both polysaccharides (1:0.6 and 1:10) and it was only at certain ALG/CS mass ratios that condensed NCs with small size were obtained. As the NCs were formed from the electrostatic interaction between negative carboxylic groups of ALG and positive amine group of CS [18], optimum amounts of polymers were needed for closer and stronger interaction. The presence of one of the polymers in excess loosened the interaction leading to larger particles [19].

**Table 1: Composition and characterization of CS/ALG NCs**

| Formula Code | ALG/CS v/v | ALG/CS w/w | pH | REP (mg/mL) [a] | PS (nm) | PI[b] | ζ [c] (mV) | EE% |
|---|---|---|---|---|---|---|---|---|
| P1 | 1:2 | 1:1.67 | 5 | --- | clear solution | NA[d] | NA | NA |
| P2 | 1:3 | 1:2.5 | 5 | --- | 259.8±3.35 | 0.38 | 30.83±2.09 | NA |
| P3 | 1:4 | 1:3.33 | 5 | --- | aggregates | NA | NA | NA |
| P4 | 1:3 | 1:2.5 | 5.5 | --- | 354.4±15.91 | 0.48 | 32.2±2.27 | NA |
| P5 | 1:3 | 1:2.5 | 6 | --- | 396.8±23.26 | 0.44 | 31.1±1.55 | NA |
| P6 | 1:3 | 1:0.6 | 5 | --- | 359.5±8.40 | 0.51 | 29.3±0.85 | NA |
| P7 | 1:3 | 1:5 | 5 | --- | 263.1±2.90 | 0.31 | 33.30±1.21 | NA |
| P8 | 1:3 | 1:10 | 5 | --- | 340.7±8.86 | 0.38 | 35.4±1.56 | NA |
| L1 | 1:3 | 1:0.6 | 5 | 0.025 | 331.3±4.36 | 0.47 | 27.4±1.51 | 51.8±2.91 |
| L2 | 1:3 | 1:2.5 | 5 | 0.025 | 311.5±2.06 | 0.47 | 26.9±1.79 | 46.40±2.11 |
| L3 | 1:3 | 1:5 | 5 | 0.025 | 299.0±9.62 | 0.51 | 27.0±1.59 | 85.87±1.00 |
| L4 | 1:3 | 1:10 | 5 | 0.025 | 310.9±21.2 | 0.46 | 29.5±2.09 | 87.91±5.07 |
| L5 | 1:3 | 1:0.6 | 5 | 0.05 | 349.9±15.94 | 0.54 | 27.6±1.21 | 15.44±4.05 |
| L6 | 1:3 | 1:2.5 | 5 | 0.05 | 295.4±13.18 | 0.52 | 28.1±1.12 | 50.99±1.10 |
| L7 | 1:3 | 1:5 | 5 | 0.05 | 375.1±3.32 | 0.42 | 27.6±2.57 | 43.92±2.50 |
| L8 | 1:3 | 1:10 | 5 | 0.05 | 359.4±10.11 | 0.48 | 31.1±1.55 | 43.12±7.45 |

[a]REP concentration in final dispersion. [b]PI: polydispersity index, [c] **ζ**:zeta potential and [d]NA: not applicable.

It is worthy to note that positive zeta potential values, ranging from 29.3 to 35.4, were obtained whatever the mass ratio of the two polyelectrolytes, probably due to the presence of CS free amino groups. Furthermore, the zeta potential increased as the mass ratio of ALG/CS was changed from 1:0.6 to 1:10 as seen in table 1. These findings corroborated with the results of a recent work on chitosan-dextran sulfate nanoparticles [19].

**Characterization of REP-loaded NCs**

Because of the amphoteric nature of REP and its ionizable nature, it was thought to incorporate the drug at two different concentrations using the previous four ALG: CS mass ratios to investigate the effect of its addition on the particles characteristics.

**Particle Size (PS)**

At low (L1-L4) and high (L5-L8) drug loading, the PS of the NCs ranged from 299 to 331 and 295.4 to 375.1 nm respectively compared to 259.8 to 359.5 nm for the blank NCs (table 1). The presence of REP, acquiring a negative charge in ALG solution (pH 6.5) might have interfered with the polymers cross-linking producing such significant increase in PS at mass ratios (1:2.5 and 1:5) in formulae L2, L3, L6 and L7. However, an opposite effect was seen at the extremes of the mass ratios of ALG to CS (at mass ratios 1:0.6 and 1:10) in formulae L1, L4, L5 and L8). Hence, at optimum charge density of the two polymers, the presence of the charged drug might have been electrostatically associated within the NCs matrix at the expense of ALG/ CS interactions resulting in larger particles. While, in the presence of excess of any of the polyelectrolytes, the drug charge contributed to the ionic cross linking especially with excess positive polyelectrolyte in our case. Similar results have been obtained with previous investigators [1,6]. Increasing REP concentration from 0.025 to 0.05 mg/mL resulted in NCs with near PS values at lower mass ratios of ALG to CS (1:0.6 and 1:2.5). However, a statistically significant increase in PS was noticed upon raising the REP amount at mass ratios of ALG to CS (1:5 and 1:10). It can be also noted that the PI values ranged from 0.42 to 0.54 similar to those previously reported in literature [6].

**Zeta Potential**

Zeta potential is the electrical potential in the double layer at the interface between a particle, which moves in an electric field, and the surrounding liquid. It is an indicator of repulsion between the particles. Positive zeta potential values ranging from +26.9 to +31.1 were obtained with all loaded particles indicating the presence of free surface amino groups of CS on the NCs which will facilitate adhesion and transport properties of the nanoparticles [20]. Furthermore, this suggests high stability essential to prevent particle aggregation. Moreover, such positive charge could facilitate their optimal intracellular distribution, lysosomal escape and perinuclear localization as previously evaluated in different cell lines [11]. As shown in table 1, the incorporation of REP resulted in non-significant effect at the low CS concentrations used (ALG/CS mass ratios of 1:0.6 and 1:2.5) while a significant reduction in **ζ** was seen at the high CS concentration (ALG/CS mass ratios of 1:5 and 1:10) irrespective of the drug concentration used.

**Encapsulation Efficiency % (EE%)**

The EE% showed great variation among formulae with values ranging from 15.44 to 87.91 %. Table 1 shows that at the low REP loading (0.025 mg/mL), non-significantly different EE% values were noticed at ALG/CS mass ratios below 1:5 (1:0.6 and 1:2.5). However, the EE% values nearly doubled by increasing the mass ratio to 1:5 and remained almost with further increase to1:10. As CS content increased at mass ratios of 1:5 and 1:10, the viscosity of the cationic solution might hinder drug escape, facilitating its engulfment inside the formed cross-linked NCs. On the other hand, at the high REP loading (0.05 mg/mL), the lowest ALG/CS mass ratio of 1:0.6 resulted in an extremely low REP association (15.44%) which considerably increased reaching a maximum at 1:2.5 mass ratio then decreased at 1:5 mass ratio. No variation in drug association was seen with further increase in CS content. It is also evident that lower EE% values were seen with the high drug loading except at the 1: 2.5 mass ratio where almost similar drug EE% values were seen at both drug levels used. It is thus clear that REP was highly associated with formulae L3 and L4 with respective EE% values of 85.87 and 87.91% and hence L3 showing optimum cross linking density with the two polymers and high EE% was selected for further investigation.

**Morphological examination**

Figure 2 shows representative figure of the morphology of CS/ALG NCs. This transmission micrograph shows discrete nanoparticles with spherical shape. It is worthy to note that the size appeared smaller compared to that observed by zetasizer. Similar observations had been reported with previous researchers [20]. This discrepancy between the two results can be explained based on

different manipulation of NCs samples. TEM imaging for CS/ALG NCs was performed on dehydrated samples, whereas photon correlation spectroscopy measures the apparent size (hydrodynamic radius) of a particle, including the hydrodynamic layers that form around the hydrophilic particles such as those composed of CS–ALG, leading to an overestimation of NCs size.

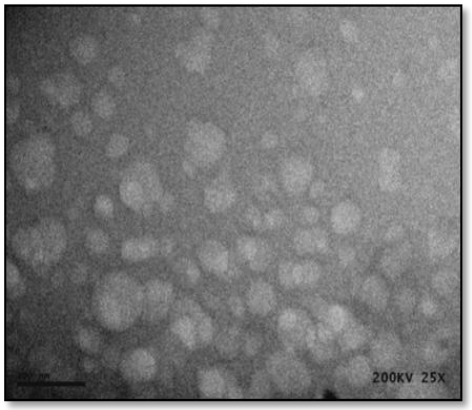


**Fig. 2: Representative TEM image of CS ALG NCS**

**Thermal analysis by DSC**

The thermal analysis of pure REP by DSC, figure 3a, revealed a single sharp endotherm at 133.28°C corresponding to its melting temperature [21]. CS, figure 3b, showed characteristic endothermic peak at 70.92°C due to loss of water linked to its amine or hydroxyl groups and an exothermic peak at 291.17°C due to the degradation of the main chain of the polymer as previously reported [22]. ALG, figure 3c, showed one endothermic peak at 67.56°C corresponding to the liberation of crystal water and another endothermic peak at 186°C which might be due to the presence of small amounts of dihydrate in the sample [23]. The exothermic peak at 239.71°C was probably due to polymer decomposition. DSC thermogram of REP:CS:ALG physical mixture was a simple superposition of the peaks of the individual components as shown in Figure 3d. REP typical melting point was absent in the representative NCs thermogram, shown in Figure 3e, indicating that the drug was molecularly dispersed in the polymer matrix.

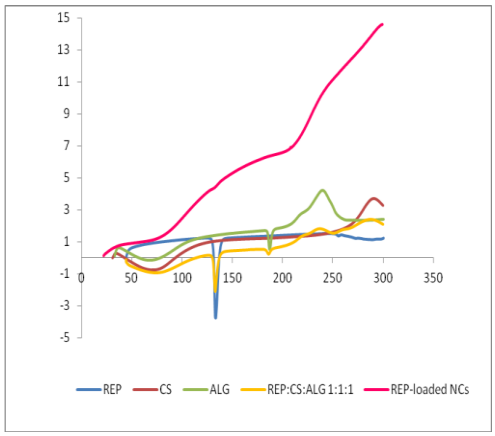


**Fig. 3: DSC thermograms of REP, CS, ALG, REP: CS: ALG physical mixture 1:1:1 and REP-loaded NCs.**

**Crystallographic assay by XRPD**

Crystallographic structures of REP, CS, ALG, and representative CS/ALG NCs were determined by X-ray diffraction (XRD) and are presented in figure 4. The diffractogram of the drug, trace a of figure 4 exhibited a series of intense peaks due to its crystalline structure. CS exhibited a specific broad peak at $2\theta$ of 25°, indicating some degree of crystallinity (figure 4b) [20]. After ionic cross-linking with ALG, no peaks were found in the diffractogram of selected CS/ALG NCs, reflecting the destruction of the native CS packing structure as seen in figure 4d[24]. CS/ALG NCs are composed of a dense network structure of interpenetrating polymer chains cross-linked to each other by ALG counter-ions. The XRD implicated greater disarray in chain alignment in the NCs after cross-linking [25]. None of the drug peaks could be seen by close examination of the diffractogram of representative NCs. Its sharp crystal peaks were overlapped with the noise of the polymers and disappeared, indicating that REP was completely and successfully encapsulated into the cores of CS/ALG NCs confirming DSC results.

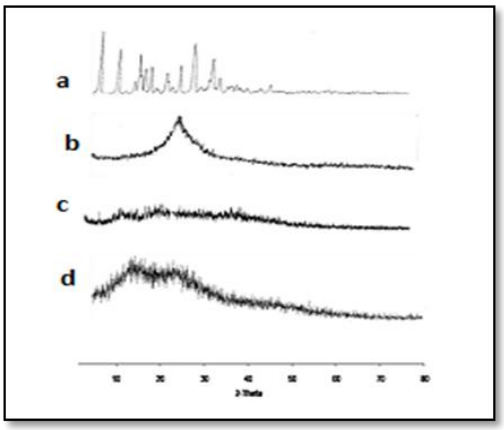


**Fig. 4: X-ray diffractograms of (a) REP, (b) CS, (c) ALG, and (d) REP-loaded NCs.**

**FT-IR**

The presence of polyhydroxy groups in CS, ALG and REP added to CS amino groups favours the formation of intermolecular hydrogen bonding and promotes the formation of ionic interactions. Several characteristic absorbance peaks can be identified in the FT-IR of pure CS (figure 5a): the characteristic peak of the hydroxyl group (OH) was recorded at 3363.8 $cm^{-1}$, high intensity peaks corresponding to carbonyl (C=O) stretching of the secondary amine (amide I band) and bending vibration of the N-H group, N-acetylated residues (amide II band) were detected at 1657.2 and 1597.2 $cm^{-1}$respectively. Peaks observed at 1422.2 and 1380.3 $cm^{-1}$ were due to the N-H stretching of the amide and ether bonds and N-H stretching (amide III band) respectively. Peaks at 1075.6 and 1031.5 were assigned to the secondary hydroxyl group and the primary hydroxyl group [6, 26]. FT-IR spectrum of ALG, figure 5b, exhibited two characteristic peaks at 3389.1 and 2936.7 $cm^{-1}$ that corresponded to hydroxyl group and O-H stretching. Peaks at 1616.8 and 1420.0 $cm^{-1}$ were assigned to symmetric COO- and asymmetric COO- stretching vibration and peak at 1069.4 $cm^{-1}$ due to vibration of the carboxylate ring [26]. In the spectrum of blank CS/ALG- NCs, figure 5c, ALG peaks were slightly shifted to lower frequencies (1616.8 to 1606.7 $cm^{-1}$ and 1420.0 to 1412.8 $cm^{-1}$) and CS amide peaks were converted into a singlet band at 1606 $cm^{-1}$ while the hydroxyl group peak, with the broad absorbance at 3366.3 $cm^{-1}$, remained almost at the same position in the formed NCs.

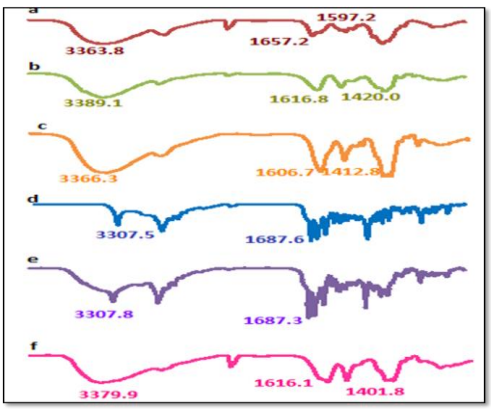


**Fig. 5 : FT-IR spectra of powders of (a) CS, (b) ALG, (c) Blank NCs, (d) REP, (e) REP: CS: ALG physical mixture 1:1:1, (f) REP-loaded NCs..**

The FT-IR spectrum of REP, illustrated in figure 5d, reveals the presence of strong absorption peaks at 3307.5 $cm^{-1}$, assigned to N-H stretching vibration, bands at 2937.2 $cm^{-1}$ (C-H stretching) and 1687.6 $cm^{-1}$ corresponding to the carbonyl group. The bands at 1445.0 and 1215.5 $cm^{-1}$ were due to the C-O stretching and O-H bending vibrations [21]. The spectrum pattern of the 1:1:1 physical mixture of CS:ALG:REP corresponded to the superposition of the IR spectra of CS, ALG and REP as seen in figure 5e. Concerning REP-loaded NCs, figure 5f, the characteristic N-H stretching vibration peak of REP 3307.5 $cm^{-1}$ almost completely disappeared together with many other drug characteristic peaks indicating the presence of strong interaction between REP and NCs matrix.

**Colloidal stability:** The data shown in table 2 reveal that, after storage of the selected NCS of formula L3 at 4ºC for seven days, no particle aggregation was noted and the dispersion exhibited its light blue opalescence and no statistically significant changes in NCs PS and PI were found. This stability could probably be due to the appropriate selected pH conditions (the final pH of the suspension was around 5), together with the high cross-linking density, small size, narrow particle size distribution and high surface potential of the particles. As stated in earlier studies, reducing the storage temperature to 4ºC or using freeze-drying with a cryoprotective agent is expected to further improve the long-term storage stability of CS nanoparticles [27].

**Table 2: Results of the stability study of formula L3 (mean ± S.D., n=3)**

| Parameter | PS (nm) | PI |
|---|---|---|
| Fresh NCs dispersion | 299.0 ± 9.62 | 0.51 |
| Stored NCs dispersion* | 315.4 ± 14.56 | 0.53 |

*Stored for 7 days at 4°C

## CONCLUSION

The NCs were prepared using a fast and gentle method of CS cross-linking with ALG. Physiochemical properties such as particle size and charge can be simply manipulated by varying the principal processing parameters such as CS volume, pH and ALG to CS mass ratio. Fabrication of plain positively charged CS/ALG NCs was evidenced by dynamic light scattering (DLS), analytical FT-IR technique and transmission electron microscopy (TEM). Molecular dispersion of REP within the NCs was observed from XRD and DSC analysis. REP loading could be modulated by careful selection of the ALG to CS mass ratio and REP concentration factors. Maximum entrapment efficiency of 85% was observed for CS/ALG NCs at ALG to CS mass ratio of 1:2.5 and 0.025 mg/mL drug concentration. The presence of the amphoteric drug REP affected greatly the size and ZP of the NCs and its effect depended greatly on the polyelectolytes mass ratio. Further studies are needed to test the *in vitro* release studies and in *vivo* performance for evaluation of their antidiabetic efficacy.

## CONFLICT OF INTEREST

The authors declare no conflict of interest.

## REFRENCES

1. Goycoolea FM, Lollo G, Lopez C, Quaglia F, Alonso MJ. Chitosan-Alginate Blended Nano particles as Carriers for the Transmucosal Delivery of Macro molecules. Bio-macro molecules 2009; 10(7): 1736–1743.
2. Meng X, Tian F, Yang J, He C, Xing N, Li F. Chitosan and alginate polyelectrolyte complex membranes and their properties for wound dressing application. J Mater Sci Mater Med 2010; 21: 1751–1759.
3. Fiebrig I, Harding SE, Davis SS. Sedimentation analysis of potential interaction between mucins and a putative bioadhesive polymer. Progr Coll Polym Sci 1994; 94: 66–73.
4. Smith JM, Dornish M, Wood, EJ. Involvement of protein kinase C in chitosan glutamate-mediated tight junction disruption. Biomaterials 2005; 26(16): 3269–3276.
5. Chae SY, Jang MK, Nah JW. Influence of molecular weight on oral absorption of water soluble chitosans. J Control Release 2005; 102: 383–394.
6. Papadimitriou S, Bikiaris D, Avgoustakis K, Karavas E, Georgarakis M. Chitosan nanoparticles loaded with dorzolamide and pramipexole. Carbo Poly 2008; 73(1): 44-54.
7. Gubbala SK. Polyelectrolyte complex: A pharmaceutical review. Int J Pharm Biol Sci 2012; 2(3): 399-407.
8. Soane RJ, Ferier M, Perkins AC, Jones NS, Davis SS, Illum L. Evaluation of the clearance characteristics of bioadhesive system in humans. Int J Pharm 1999; 178: 55-65.
9. Brooking J, Davis SS, Illum L. Transport of nanoparticles across the rat nasal mucosa. J Drug Target. 2001; 9: 267– 279.
10. United States Patent, Sung H-W, Liang H-F, Tu H. Nanoparticles for paracellular drug delivery, Patent No 7,265,090 2007.
11. Yue Z-G, Wei W, Lv P-P, Yue H, Wang L-Y, Su, Z-G, Ma G-H. Surface Charge Affects Cellular Uptake and Intracellular Trafficking of Chitosan-Based Nanoparticles. Biomacromolecules 2011; 12(7): 2440-2446.
12. Grell W, Hurnaus R, Griss G. Repaglinide and related hypoglycemic benzoic acid derivatives. J Med Chem. 1998; 41: 5219-5246.
13. Makino C, Sakai H, Yabuki A. Nateglinide controlled release tablet containing compressionable enteric coated granules. Chem Pharm Bull 2010; 58(9): 1136-1141.
14. Lund SS, Tarnow L, Stehouwer CDA, Schalkwijk CG, Frandsen M, Smidt UM, Pedersen O, Parving HH, Vaag A. Targeting hyperglycaemia with either metformin or repaglinide in non-obese patients with type 2 diabetes: results from a randomized crossover trial. Diabetes Obes Metab 2007; 9(3): 394-407.
15. Jain S, Saraf S. Repaglinide-loaded long-circulating biodegradable nanoparticles: Rational approach for the management of type 2 diabetes mellitus. J Diabetes 2009; 1(1): 29-35.
16. Fan W, Yan W, Xu Z, Ni H. Formation mechanism of monodisperse, low molecular weight chitosan nanoparticles by ionic gelation technique. Colloids Surf B Biointerfaces 2012; 90: 21– 27.
17. Simsek-Ege FA, Bond GM, Stringer J. Polyelectrolye Complex Formation Between Alginate and Chitosan as a Function of pH. J Appl Polym Sci 2003; 88: 346–351.
18. Ribeiro AJ, Silva C, Ferreira D, Veiga F. Chitosan reinforced alginate microspheres obtained through the emulsification/internal gelation technique. Eur J Pharma Sci 2005; 25(1): 31-40.
19. Katas H, Raja MA, Lam KL. Development of chitosan nanoparticles as a stable drug delivery system for protein/siRNA. Int J Biomat 2013;1-9.
20. Mahmoud AA, El-Feky GS, Kamel R, Awad GEA. Chitosan/sulfobutylether-B-cyclodextrin nanoparticles as a potential approach for ocular drug delivery. Int J Pharm 2011; 413: 229-236.
21. Aramă C, Nicolescu C, Nedelcu A, Monciu C-M. Synthesis and characterization of the inclusion complex between repaglinide and sulfobutylether-β-cyclodextrin (Captisol®). J Inc Phenom and Macrocyclic Chem 2011; 70(3-4): 421-428.
22. Ventura CA, Tommasini S., Crupi E, Giannone I, Cardile V, Musumeci T, Puglisi G. Chitosan microspheres for intrapulmonary administration of moxifloxacin: Interaction with biomembrane models and *in vitro* permeation studies. Eur. J. Pharm. Biopharm. 2008; 68: 235-244.
23. Shabbeer S, Shaheeda, & Ramanamurthy, KV. Formulation and evaluation of chitosan sodium alginate microcapsules of 5-fluorouracil for colorecal cancer. Int J Res Pharm Chem 2012; 2(1): 7-19.

24. Yoksan R, Jirawutthiwongchai J, Arpo K. Encapsulation of ascorbyl palmitate in chitosan nanoparticles by oil-in-water emulsion and ionic gelation processes. Colloids Surf B Biointerfaces 2010; 76: 292-297.
25. Qi L, Xu Z, Jiang X, Hu C, Zou X. Preparation and antibacterial activity of chitosan nanoparticles. Carbohyd Res 2004; 339: 2693-2700.
26. Li P, Dai Y, Zhang J, Wang A, Wei Q. Chitosan-Alginate nanoparticles as a novel drug delivery system for nifedipine. Int J Biomed Sci 2008; 4(3): 221-228.
27. Morris GA, Castile J, Smith A, Adams GG, Harding SE. The effect of prolonged storage at different temperatures on the particle size distribution of tripolyphosphate (TPP)–chitosan nanoparticles. Carbohyd Polym 2011; 84: 1430–1434.